# Tunneling microscopy from 300 to 4.2 K

by S. A. Elrod

A. Bryant

A. L. de Lozanne

S. Park

D. Smith

C. F. Quate

A scanning tunneling microscope (STM) has been developed for operation over the full temperature range from 300 to 4.2 K. At room temperature, the instrument has been used to produce topographic images of grain structure in a copper-titanium alloy foil and of atomic structure on a Pt(100) surface. At low temperatures, the instrument can be used in a new spectroscopic mode, one which combines the high spatial resolution of the STM with the existing technique of electron tunneling spectroscopy. This new capability has been demonstrated by using the microscope to probe spatial variations in the superconducting character of a niobium-tin alloy film.

#### Introduction

While the use of tunneling for microscopy is a fairly recent development, its use as a spectroscopic tool underlies several well-established fields. In the case of tunneling spectroscopy, however, electron flow has conventionally been between planar electrodes separated by a solid insulating barrier. At low temperatures, the current-voltage (*I-V*) characteristics of such sandwich tunnel junctions are found to be rich in spectroscopic information. This information has been successfully related to such diverse physical phenomena as superconductivity of the electrodes [1], inelastic tunneling associated with photons, phonons, or molecular excitations [2], and resonant tunneling through barrier states [3]. All of

<sup>®</sup>Copyright 1986 by International Business Machines Corporation. Copying in printed form for private use is permitted without payment of royalty provided that (1) each reproduction is done without alteration and (2) the *Journal* reference and IBM copyright notice are included on the first page. The title and abstract, but no other portions, of this paper may be copied or distributed royalty free without further permission by computer-based and other information-service systems. Permission to *republish* any other portion of this paper must be obtained from the Editor.

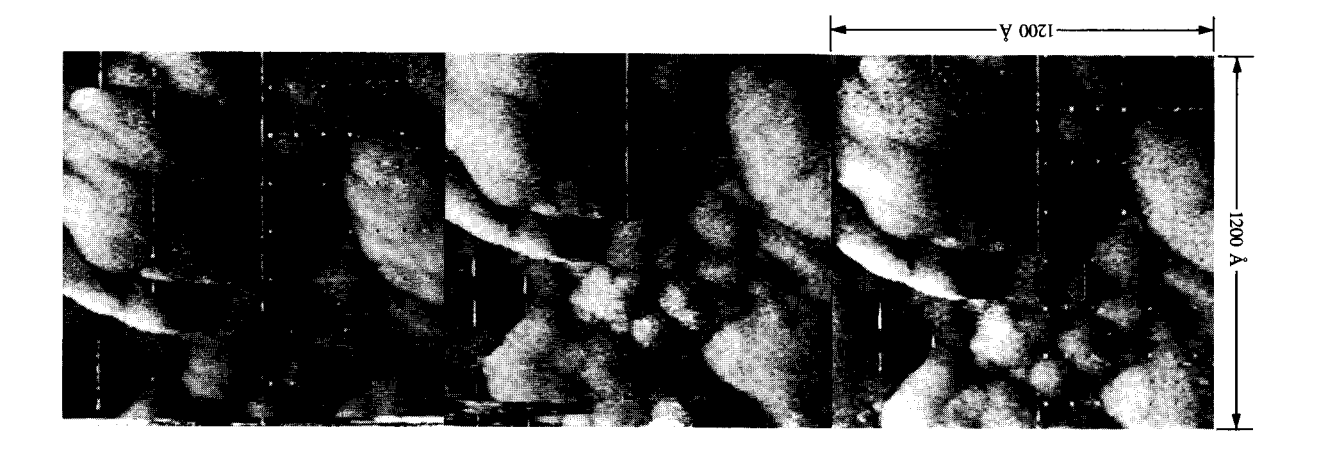
these phenomena have characteristic energies below several hundred millielectron volts; low temperatures (≤4.2 K) are therefore required to reduce thermal smearing to an acceptable level.

A major disadvantage of conventional planar structures is that the desired spectroscopic information is spatially averaged over the full area of the junction. While junctions as small as 1200 × 3000 Å have been fabricated [4], these dimensions are still considerably larger than the characteristic length over which properties of interest might be expected to vary. For the case of superconductors, the relevant scale is set by the coherence length, which can range from thousands to tens of angstroms. For resonant or inelastic tunneling, large variations can be expected to occur over the size of a single molecule. Conventional tunnel junctions also suffer from the liability that the interpretation of results can be confused by unwanted effects of the nonideal solid tunneling barrier.

The low-temperature tunneling microscope described in this paper was developed in order to capitalize on the demonstrated lateral resolution of the scanning tunneling microscope and to combine it with the powerful and well-established technique of tunneling spectroscopy. It was hoped that the resulting instrument would allow for the possibility of spectroscopic studies of surfaces with a lateral resolution approaching atomic dimensions. In addition to very high lateral resolution, the low-temperature tunneling microscope would offer the advantage of an ideal (vacuum) barrier. The instrument would also afford easy access to the electrodes, making possible the introduction of molecular species for inelastic tunneling spectroscopy [2].

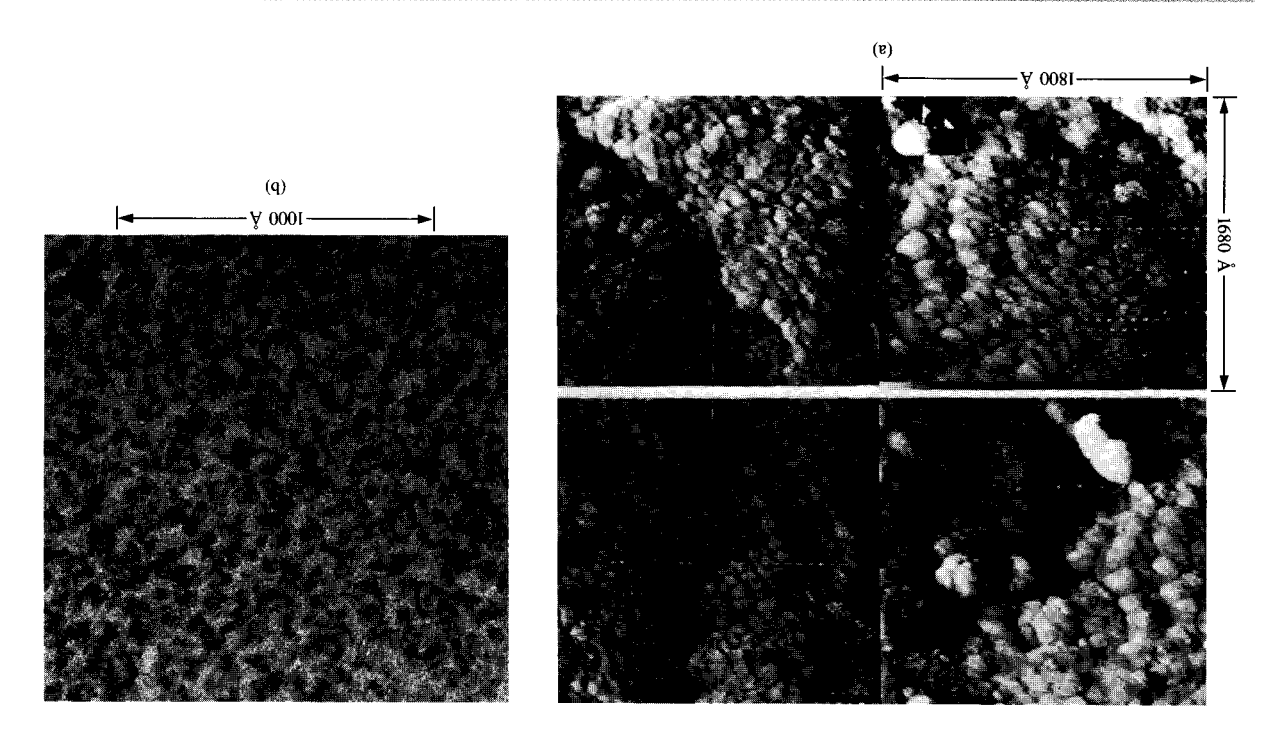
### Room-temperature studies

During the development of the low-temperature instrument, several room-temperature studies were conducted. The exponential dependence of tunneling current on



LEJDÔJ-I

Three topographic images of the same region of a copper-titanium alloy foil. The images were taken in rapid succession to demonstrate reproducibility.



z sinfis

(a) STM images of four different portions of the surface of the copper-titanium foil. (b) TEM image of a similar copper-titanium foil.

check on such important attributes as resolution and image reproducibility. STM images of grain structure in a coppertisanium alloy foil compared favorably with TEM images.

interelectrode spacing was verified [5]. As a check on microscope performance, topographic studies of several metal surfaces were made. These studies provided a valuable

Images of a single-crystal surface of Pt(100) showed reproducible features with atomic resolution ( $\approx$ 3 Å). Details of the topographic mode of STM operation are described elsewhere [5–7].

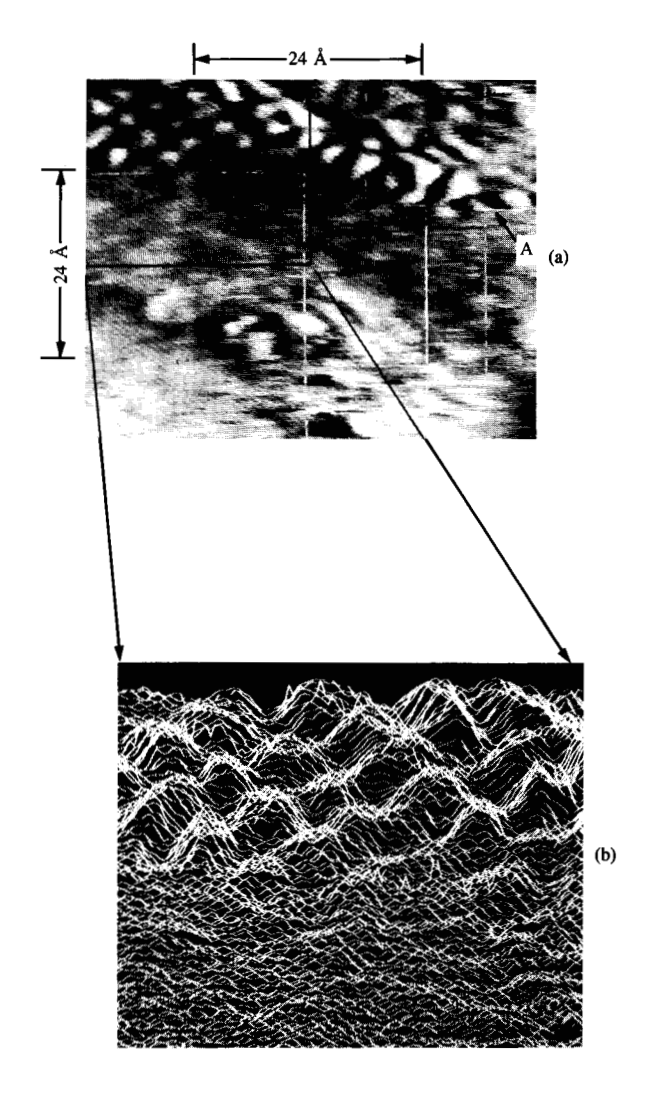
An alloy foil of copper and titanium [8] exhibited very rich structure under topographic examination with the STM. As described elsewhere [8], the sample was prepared by cosputtering copper and titanium to form an amorphous film of  $Cu_{60}Ti_{40}$ . The film was annealed at 418°C and quenched into a metastable microcrystalline phase having a characteristic grain size of  $\approx$ 60 Å.

The sample was imaged at a gap resistance of 250 k $\Omega$  with a tungsten tip at a dc tip voltage of -1.5 mV. It was argonion-beam-milled (500 V at 0.26 mA/cm<sup>2</sup> for two minutes), then transferred in air to the STM. Imaging was accomplished at  $10^{-7}$  torr the following day. Images were taken in four minutes with a 1-Hz line rate. Image quality seemed to improve after the tip was touched to the surface with an applied voltage of -30 V and then "walked" to a new location. To compensate for an overall tilt of the sample, data were ac coupled to a significant degree. The z calibration therefore depended on the data frequency and is not included.

Figure 1 shows three images taken in rapid succession. The images show high sensitivity to grain structure and are very reproducible. Shown in Figure 2(a) are four STM images taken at different locations on the surface. For comparison, a TEM image of a similar sample [8] has been included in Figure 2(b). We note that while the TEM averages over the entire sample thickness, the STM is surface-sensitive only.

The capability of the STM to resolve atomic features was demonstrated using a platinum sample having a (100) surface. The sample was prepared by cleaning in solvents and then heating in vacuum to approximately 800°C at a pressure of  $10^{-8}$  torr. The tunneling tip was "prepared" by touching it to the surface with an applied voltage of -30 V. The sample was imaged at a gap resistance of 250 k $\Omega$  and a dc tip voltage of -25 mV. As was the case with the images from the copper-titanium sample, data were ac coupled; the z calibration is therefore not included.

Figure 3(a) shows a region of the platinum surface. The upper left portion of the image shows a square array of atomlike features. The average nearest-neighbor distance is measured to be 3.2 Å. This portion of the image is also depicted in Figure 3(b) in the more conventional amplitude trace format. The expected nearest-neighbor distance for an unreconstructed surface of Pt(100) is 2.8 Å. The discrepancy with the measured value of 3.2 Å is within the calibration error of the piezoelectric drives. While it is tempting to identify the square array as the platinum lattice, several cautions are in order. The cleaning procedure which we adopted was modest and is known to leave residual carbon on the surface [9]. In addition, we acknowledge that none of



212181818

(a) Region of a Pt(100) surface. A square array of atomlike features is identified in the upper left corner. The average nearest-neighbor distance is 3.2 Å. At location A, a discontinuity is indicated, possibly due to tip switching. (b) Top left corner of (a) is depicted in the more conventional amplitude trace format.

the conventional tools (Auger, LEED) was used to ascertain the degree of surface order and cleanliness. While the measurements are thus nonideal, they nevertheless demonstrate that atomic resolution has been achieved.

Figure 4 shows two images taken in rapid succession to verify that the observed atomic features are reproducible. Each image was obtained in 50 seconds. One feature has been selected; it is indicated by arrows in the images. The displacement of atomic features is believed to be due to thermal drift or piezoelectric creep.

Image interpretation is not always as straightforward as the above results might suggest. In particular, we recognize

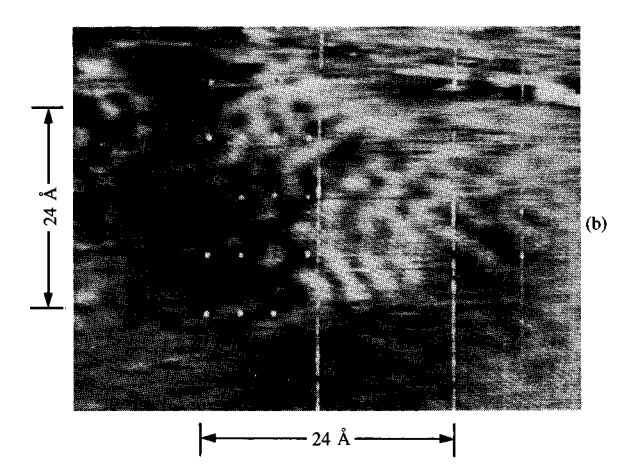


# Figure 4

Two consecutive images of the same area of a Pt(100) surface. A feature which can be seen in both images is identified by arrows.

two problems, both associated with the unknown geometry of the tunneling tip. The first is the fundamental problem involved in trying to separate the effects of an unknown tip geometry from those due to surface topography. One can even imagine the extreme case in which a very flat tip is itself imaged by a sufficiently rough surface. The most desirable situation is clearly one in which the surface is atomically flat.

The second problem is associated with the switching of tunneling current between minitips [6]. For a tip with a sufficiently flattened end, switching might even occur between minitips located microns apart. Tip-switching effects have been intermittently observed in most of the topographic studies conducted by our group. In images, these appear as abrupt boundaries between regions which seem unrelated. The effects are most pronounced after the tip has been moved to a new location on the sample, and they seem to decrease with time. For the images presented in this paper (with the possible exception of Figure 3), tip-switching effects are believed to be absent.

# Low-temperature studies [10]

The low-temperature tunneling microscope (LTTM) offers the first opportunity to conduct spectroscopic studies of surfaces with a lateral resolution approaching atomic dimensions. Of all the physical phenomena which can give rise to identifiable spectroscopic features in the tunneling *I-V* characteristic, superconductivity of the electrodes has one of the largest and most distinctive signatures. Superconductive tunneling was therefore chosen as the first spectroscopy with which to test the capabilities of the new instrument.

For two reasons, the surface of superconducting Nb<sub>3</sub>Sn was selected as the one to be studied. First, independent measurements [11] indicated the possible presence of microscopic spatial inhomogeneities, which would provide a contrast mechanism for spectroscopic imaging. Second, the energy gap of Nb<sub>3</sub>Sn is among the largest known (3.3 mV) [11] and should be readily discriminated in the tunneling *I-V* characteristic.

As a normal tip is scanned over the superconducting Nb<sub>3</sub>Sn surface, a single parameter is extracted from the *I-V* characteristic to provide a direct measure of the local superconductivity. Images produced in this fashion show strong spatial variations, with reproducible transitions between fully normal and fully superconducting behavior on length scales as small as 13 nm. Images taken above and below the critical temperature confirm that the observed effects are due to superconductive tunneling. Additional confirmation comes from a successful fit of the measured *I-V* curves to a simple superconductor–insulator–normal metal (SIN) tunneling model [7].

Poppe and Schroder [12] have developed an apparatus similar to the LTTM described in this paper. We also acknowledge the low-temperature tunneling work of Moreland et al. [13], who use flexible substrates to control the interelectrode spacing. In both cases, the authors obtain excellent tunneling characteristics, although in neither case has a scanning capability (i.e., microscopy) yet been demonstrated.

#### • Spectroscopic imaging

The *I-V* characteristic of an SIN junction can provide detailed information on the properties of the superconducting electrode [1]. With respect to the ohmic case, the most pronounced alteration in the *I-V* characteristic is associated with a gap in the excitation density of states of the superconductor.

For spatially resolved LTTM studies of superconductivity, one would ideally like to measure the full *I-V* curve at every point on the sample surface. The local value of the energy gap could then be deduced by fitting the individual *I-V* curves to a simple SIN tunneling model [1, 6]. For this pilot study of the LTTM's capabilities, however, a simplified approach was taken.

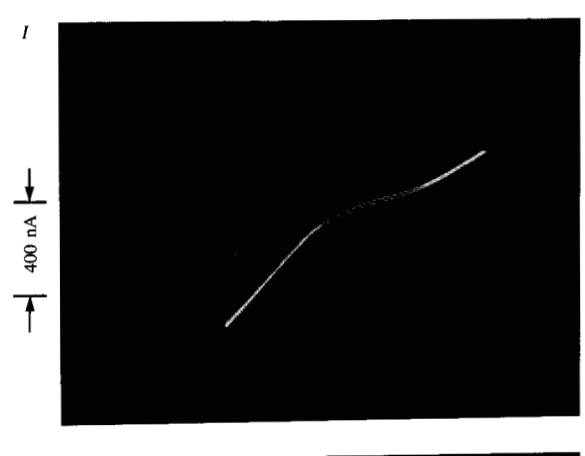
For spectroscopic studies, the gap voltage is triangle-wave modulated at 1 kHz. The analog time derivative of the junction current (dI/dt) is displayed as a function of junction voltage, yielding a sensitive measure of the local electronic structure but differing from the conventional dynamic conductance (dI/dV) by a factor of dV/dt. At the same time that the I-V curve is being swept at 1 kHz, the ac current is detected with a lock-in amplifier to provide a signal proportional to the gap resistance averaged over the full I-V curve. This signal is further amplified to provide feedback to the piezoelectric drive which controls the interelectrode spacing. Since the 1-kHz sweep rate is fast compared to the feedback response, the only effect of the latter is to stabilize the average gap resistance at the desired equilibrium value.

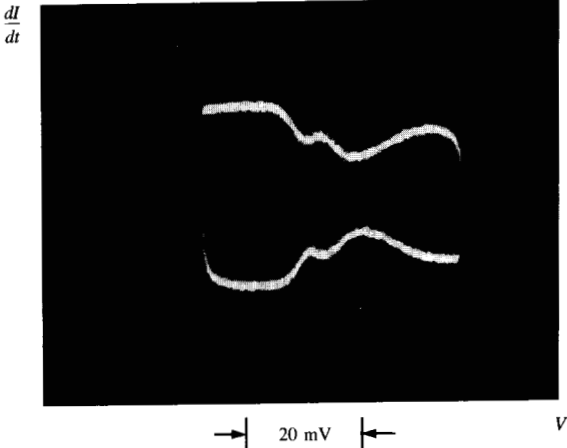
As the tip is scanned laterally, the magnitude of dI/dt changes with variations in superconductivity and/or topography. Some care must therefore be taken to sort out the different effects on the tunneling current. In order to obtain a spectroscopic image of the sample, we choose to extract a *single* parameter from the I-V curve which is a direct measure of the local superconductivity but excludes the effects of changing topography. This is accomplished by sampling the zero-bias value of dI/dt and normalizing it to the average gap resistance.

We justify this particular choice of spectroscopy signal in the following way. We assume that the basic physics of the tunneling process, and hence the shape of the I-V characteristic curve, remains unchanged as the gap resistance varies (due to topography) about its equilibrium value. In a simple SIN tunneling model, the normal state resistance enters the problem only as an overall normalization factor. With the assumptions noted above, the normalization procedure yields a signal which equals unity for normal metal-insulator-normal metal (NIN) junctions (independent of topography) and zero for ideal SIN junctions at T = 0. A more detailed justification for this procedure is given in [6].

# • LTTM results for Nb, Sn

In order to minimize the oxide contribution to the tunneling barrier, iridium was used for the normal metal tip. The sample which was examined was a thin film of Nb<sub>3</sub>Sn with an inductively measured critical temperature of 18 K. To reduce the possibility of lattice damage (and resultant degradation of superconductivity) from the cleaning procedure, the sample was not ion-milled as in previous experiments [5], but rather was briefly etched in a 10% aqueous solution of HF immediately before being installed in the tunneling unit. Following pumpdown and cooling to 4.2 K, helium exchange gas was introduced into the vacuum space (resulting in a pressure increase to  $5 \times 10^{-5}$  torr). Cold-plate baffles ensured that only helium gas reached the sample. Tunneling measurements were made in the exchange gas.





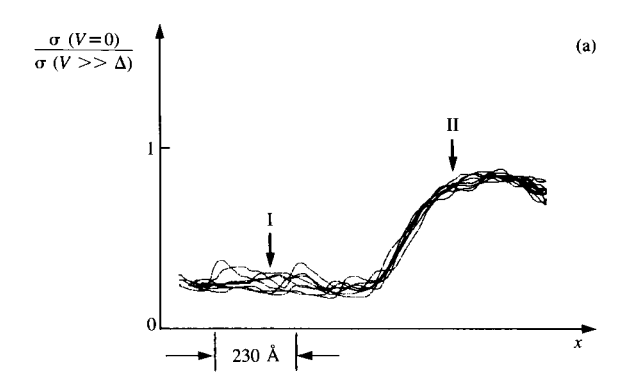
Flaure 5

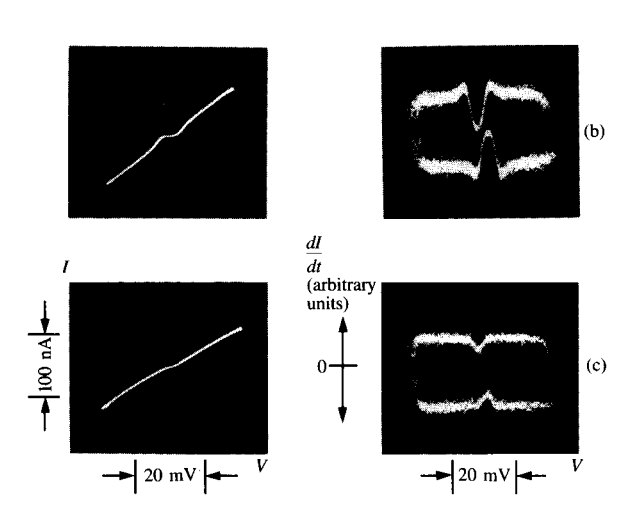
Prior to tip cleaning: Traces of I vs. V and dI/dt vs. V for a Nb<sub>3</sub>Sn sample and an iridium tip at a temperature of 6 K.

Prior to the tip-cleaning procedure described below, I-V curves were unstable, with gross features superimposed on the less pronounced (if present) superconducting gap. Maxima and minima in dI/dt at voltages from 0 to 100 mV, along with either sign of overall second derivative, were measured. Similar effects were observed for nonsuperconducting samples. The I-V characteristic in Figure 5 is representative of the type frequently encountered. The figure shows both I vs. V and dI/dt vs. V for a Nb<sub>3</sub>Sn sample and an iridium tip at a gap resistance of 50 k $\Omega$  and a temperature of 6 K.

The superconducting gap of Nb<sub>3</sub>Sn is expected to be in the range of 2.3 to 4.5 mV [11]. Any gap structure present in Figure 5 is totally obscured by background distortions of the I-V characteristic. Similar effects were observed at gap resistances up to 1 M $\Omega$ , and for different sample and tip materials. I-V characteristics of the type shown in Figure 5 were unstable, changing among a myriad of different shapes on a time scale of seconds.







## Bollias

(a) Repeated spectroscopic (normalized zero-bias conductance) linescans over a region of the Nb<sub>3</sub>Sn sample, showing a continuous spatial transition between normal and superconducting behavior. (b) and (c) *I-V* characteristics corresponding to locations I and II.

Possible explanations for the observed I-V characteristics include (1) low effective barrier height, (2) resonant tunneling, and (3) inelastic tunneling. In the first case, we refer to nonohmic contributions to the tunneling current which become significant when the applied voltage is no longer much less than the barrier height [14]. Very low barrier heights ( $\approx$ 0.1 eV) would result in nonlinear behavior at the low voltages shown in Figure 5. Such barrier heights have been intermittently observed with the STM [6]; their origin is not well understood. In any case, the simple explanation of low barrier height would only account for a monotonic increase in the dynamic conductance about its minimum value.

The second possibility is that of resonant transmission through an impurity situated somewhere between the tunneling electrodes [3]. Field-emission studies [15] of

resonant tunneling through adsorbed species suggest that large effects on the I-V characteristic are to be expected. Observed time-dependent effects in the STM would correspond to the migration of molecules on the sample or tip, possibly under the influence of the high electric field ( $10^7$  V/m) near the tip. The helium exchange gas used in these experiments may have participated in such resonant tunneling effects.

The third possibility is that of inelastic tunneling associated with the excitation of vibrational modes of molecules situated between the tip and surface. For planar junctions [2], inelastic tunneling spectra show peaks which agree closely with known infrared and Raman-mode energies. Conductance changes of ≤1% are observed for monolayer impurity coverage on planar junctions. Enhancement by a factor of three has recently been predicted for the STM [16]. This is still too small to account for the observed structure in Figure 5.

At moments of particular stability, *I-V* curves could be made to change reproducibly and continuously among different shapes by scanning the tip laterally. Changes of this type occurred down to scan sizes of several angstroms, providing partial evidence that the observed effects were due to single atoms or molecules.

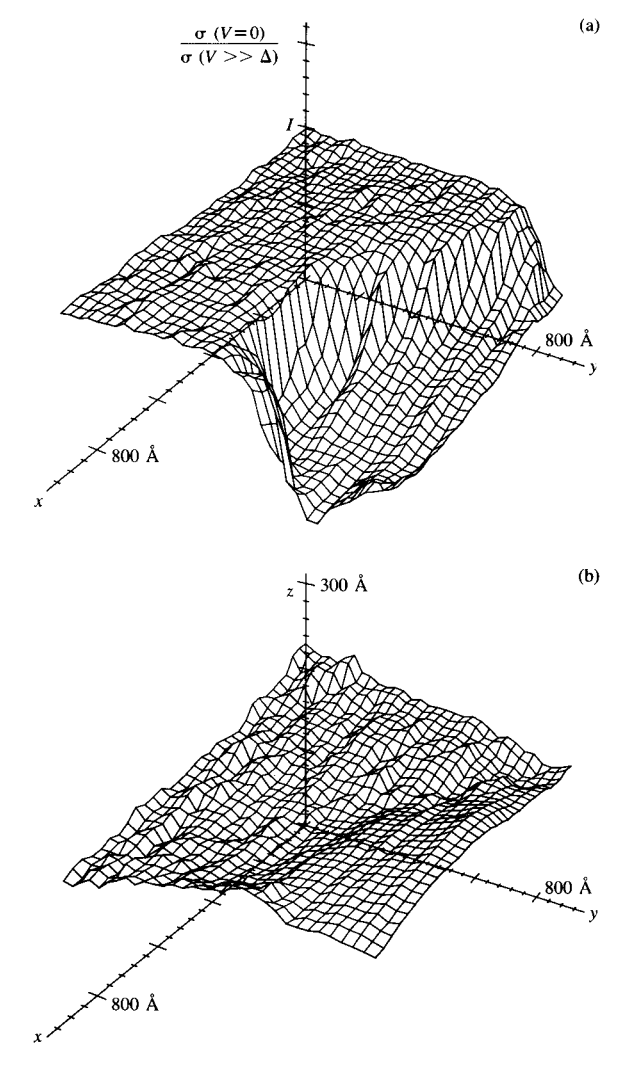
While these effects are very interesting and deserve further study, they tend to wreak havoc on any effort to obtain spectroscopic images of superconductivity. The imaging technique described above assumes an ohmic *I-V* characteristic for voltages significantly greater than the superconducting gap. *I-V* characteristics like that shown in Figure 5 would give wildly varying spectroscopic image signals having no relationship to the local superconductivity.

A tip-cleaning procedure was used to eliminate such effects. With -30 V applied to the tip, the gap spacing was reduced until current flowed. Initially, the current would increase uncontrollably, reaching the resistor-limited value of  $1.2~\mu A$ . After several attempts, it became possible to control the current at 200 nA. The current was maintained at this value for several minutes. I-V curves taken after this procedure were stable and essentially ohmic. However, the procedure resulted in the extinction of superconductivity over the full field of view of the scanner ( $2000 \times 2000$  Å). It was therefore necessary to move the tip to a new location with the magnetic walker [17] in order to observe superconducting features. Results reported in the remainder of this paper were taken after using that tip-cleaning procedure.

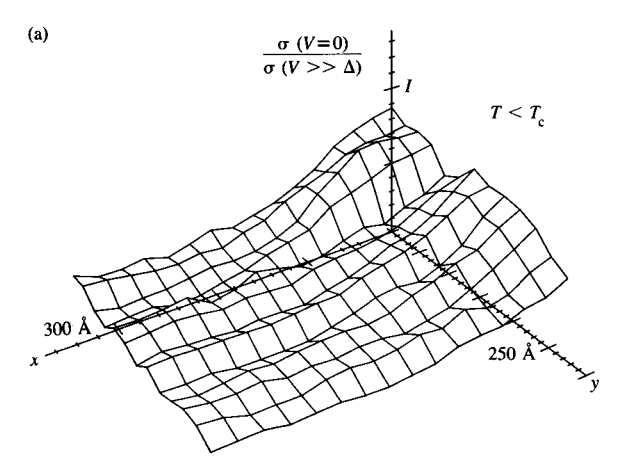
Shown in Figure 6 are repeated spectroscopic line-scans over a region of the sample, generated using the spectroscopic signal extraction technique described above. They show a continuous spatial transition between normal and superconducting regions which occurs over a distance of 230 Å. This is larger than, and therefore consistent with, the coherence length of Nb<sub>3</sub>Sn ( $\approx$ 40 Å). *I-V* characteristics for

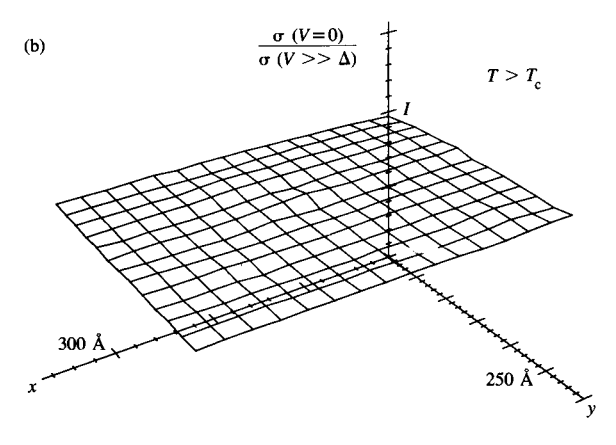
locations I and II are shown in the figure, as are the time derivatives used to obtain the spectroscopic signal.

Shown in Figure 7 is a full x-y image of the spatial variations of superconductivity over a region of the Nb<sub>3</sub>Sn surface. For this image, scanning was in the x direction; each x line-scan was taken 20 times and signal-averaged by computer. Images taken in immediate succession show excellent reproducibility; rotation of the scanning direction by 90 degrees did not alter the image appreciably. Also shown in the figure are topographic data which were obtained concurrently. The spectroscopic image shows a



(a) Full *x-y* images of the superconducting character of the Nb<sub>3</sub>Sn sample. The distance between successive grid lines is 27 Å. The vertical axis is the normalized zero-bias conductance, as discussed in the text. (b) Topographic data obtained concurrently.





Spectroscopic images obtained (a) below and (b) above the critical temperature.

transition between normal and superconducting regions which is defined by an arc in the x-y plane. The topographic image shows a similar boundary between the two regions; the superconducting region appears topographically flat, while the normal region shows more texture. Possible explanations for observed variations are discussed below. We note that a significant fraction of the data for Nb<sub>3</sub>Sn do not show such variations, but rather show exclusively superconducting or normal behavior.

Figure 8 shows spectroscopic images taken over a region of the sample below and above its critical temperature. Taken at 6.2 K, part (a) shows a distinct transition between normal and superconducting regions. Warming the sample above 20 K with a resistive heater resulted in the spectroscopic image shown in part (b). This figure demonstrates the success of the spectroscopic signal extraction technique in normalizing out topographic variations.

## • Possible causes for observed variations

There are several possible causes for the spatial variations of superconductivity observed in this sample. The first is the presence of microscopic inhomogeneities on a scale of less than 1  $\mu$ m. The presence of such inhomogeneities is suggested by heat capacity measurements [18], which show a spread in the transition temperature of niobium-tin samples. This is an unlikely explanation for the sample (25 at% Sn) used in these studies, however, because it is outside the composition range (20 at% to 24 at% Sn) for which a spread in  $T_c$  is observed.

On the other hand, the best tunnel junctions fabricated using stoichiometric Nb<sub>3</sub>Sn films still show a large spread in the superconducting gap (2.3 mV to 4.1 mV) [11]. The origin of this spread is not understood, but it can be successfully modeled by assuming the presence of microscopic domains having a distribution of energy gaps [11].

The second possibility is gap anisotropy [19], which would introduce spatial variations due to the different orientations of neighboring microcrystals. This cannot, however, explain the full variation between normal and superconducting behavior depicted in Figure 7. Furthermore, the Nb<sub>3</sub>Sn films used in this study typically grow with a preferred [200] orientation normal to the substrate [11]. Tunneling therefore proceeds along that direction unless there is substantial texture on the surface.

The last possibility is that the variations are due to damage created either by previous ion milling [5] or by the tip-cleaning procedure described above. The latter is perhaps the most likely current explanation, since the superconductive tunneling is locally extinguished after tip cleaning.

It should be emphasized that regardless of the cause of the variations observed on this sample, the results demonstrate a direct measurement of the superconducting gap on a scale two to three orders of magnitude finer than previous techniques.

### **Acknowledgments**

We thank F. Hellman, A. F. Marshall, and S. Park for generously contributing samples for these studies. This research was sponsored by the IBM Corporation, the Defense Advanced Research Projects Agency, the Office of Naval Research, and the Joint Services Electronics Program.

## References and note

- L. Solymar, Superconductive Tunneling and Applications, Wiley-Interscience Publishers, New York, 1972.
- Tunneling Spectroscopy, P. K. Hansma, Ed., Plenum Press, New York, 1982.
- S. J. Bending and M. R. Beasley, *Phys. Rev. Lett.* 55, 324 (1985); M. Ya. Azbel, *Solid-State Commun.* 45, No. 7, 527 (1983).
- C. T. Rogers and R. A. Buhrman, *IEEE Trans. Magnetics* MAG-19, No. 3, 453 (1983).

- S. Elrod, A. L. de Lozanne, and C. F. Quate, Appl. Phys. Lett. 45, No. 11, 1240 (1984).
- Scott Alan Elrod, Ph.D. Thesis, Stanford University, California, 1985.
- 7. A. L. de Lozanne, S. A. Elrod, and C. F. Quate, *Phys. Rev. Lett.* **54**, No. 22, 2344 (1985).
- A. F. Marshall, Y. S. Lee, and C. A. Stevenson, *Acta Metall.* 31, No. 8, 1225 (1983).
- 9. J. L. Gland and G. A. Somorjai, Surf. Sci. 38, 157 (1973).
- Sections of this paper have been excerpted from Ref. [7] and from A. L. de Lozanne and S. A. Elrod, *Bull. Amer. Phys. Soc.* 30, No. 3, 322 (1985).
- D. Rudman, F. Hellman, R. H. Hammond, and M. R. Beasley, J. Appl. Phys. 55, No. 10, 3544 (1984); D. Rudman, Ph.D. Thesis, Stanford University, California, 1982.
- 12. U. Poppe and H. Schroder, Proceedings of the 17th Conference on Low-Temperature Physics LT-17, 835 (1984).
- 13. J. Moreland, S. Alexander, M. Cox, R. Sonnenfeld, and P. K. Hansma, *Appl. Phys. Lett.* 43, No. 4, 387 (1983).
- J. Simmons, J. Appl. Phys. 34, No. 6, 1793 (1963) and J. Appl. Phys. 34, No. 9, 2581 (1963).
- 15. J. W. Gadzuk, Phys. Rev. B 1, 2110 (1970).
- G. Binnig, N. Garcia, and H. Rohrer, *Phys. Rev. B* 32, No. 2, 1336 (1985).
- Douglas P. E. Smith and Scott A. Elrod, Rev. Sci. Instrum. 56, No. 10, 1970 (1985).
- F. Hellman, D. A. Rudman, S. R. Early, and T. H. Geballe, *Bull. Amer. Phys. Soc.* 27, 347 (1982).
- 19. Anisotropy Effects in Superconductors, H. W. Weber, Ed., Plenum Press, New York, 1977.

Received July 2, 1985; accepted for publication November 8, 1085

Scott A. Elrod Xerox Corporation, Palo Alto Research Center, Palo Alto, California 94304. Dr. Elrod received an A.B. degree in physics from Earlham College, Richmond, Indiana, in 1981 and a Ph.D. in applied physics from Stanford University, California, in 1985. His Ph.D. research was directed toward the development of a low-temperature tunneling microscope. Dr. Elrod is currently a Visiting Scientist at the Xerox Palo Alto Research Center.

Andres Bryant Edward L. Ginzton Laboratory, Stanford University, Stanford, California 94305. Mr. Bryant received a B.S.E.E. in 1982 from the University of Maine at Orono and an M.S.E.E. in 1984 from Stanford University, California. He is currently working toward a Ph.D. in electrical engineering at Stanford. He was a recipient of IBM fellowships in 1983 and 1984. Mr. Bryant's research interests include the scanning tunneling microscope and its application to mass storage and nanolithography.

Alex L. de Lozanne Department of Physics, University of Texas at Austin, 200 West 21st Street, Austin, Texas 78712. Dr. de Lozanne is an Assistant Professor. Previously he held the Chodorow Fellowship in Applied Physics at Stanford University, under which this work was done. His Ph.D. thesis (Stanford University, California, 1982) on high-critical-temperature Josephson devices was directed by Professor M. R. Beasley. He received his bachelor's degree with highest distinction from Purdue University, Lafayette, Indiana, in December 1976. His academic honors include the Danforth, IBM, and Chodorow fellowships, the R. W. King Award, and election to Phi Beta Kappa, Phi Kappa Phi, and Sigma Pi Sigma.

**Sang-II Park** Edward L. Ginzton Laboratory, Stanford University, Stanford, California 94305. Mr. Park received a B.S. in physics from Seoul National University, Seoul, Korea, in 1981. He is currently a Ph.D. candidate in applied physics at Stanford, working on room-temperature STM especially directed toward surface physics.

**Douglas P. E. Smith** Edward L. Ginzton Laboratory, Stanford University, Stanford, California 94305. Mr. Smith received his A.B. in 1981 from Dartmouth College, Hanover, New Hampshire, and worked from 1981 to 1983 at the IBM Thomas J. Watson Research Center. Since 1982 he has been a doctoral student in the Applied Physics Department at Stanford. His present research concerns low-temperature scanning tunneling microscopy and the use of field ion microscopy to clarify the nature of the STM tip.

Calvin F. Quate Edward L. Ginzton Laboratory, Stanford University, Stanford, California 94305. Dr. Quate is a Professor of Applied Physics and Electrical Engineering. He received a B.S. degree in 1944 from the University of Utah, Salt Lake City, and a Ph.D. degree in 1950 from Stanford University, California, both in electrical engineering. In 1984 he became a Senior Research Fellow at Xerox Corporation, Palo Alto Reseach Center. Dr. Quate is a member of the American Physical Society, the National Academy of Engineering, and the National Academy of Sciences. He is a Fellow of the Acoustical Society, the American Academy of Arts and Sciences, and the Institute of Electrical and Electronics Engineers; and an Honorary Fellow of the Royal Microscopical Society. He was awarded the IEEE Morris N. Liebmann Award in 1981 and the Rank Prize for Opto-Electronics in 1982. His research interests include imaging, scanning microscopy, and new concepts for data storage.